Optical Pumping of Rubidium

Maya Desai, Jacob Shin

March 24, 2024

Abstract

We conducted optical pumping experiments on a sample of rubidium, enabling observation of its zero field resonance and Zeeman field splitting for the isotopes Rb85 and Rb87. Our estimate for the collision cross-section of the photon beam with the Rb sample was 1.2×10^{-16} m^2, compared to the theoretical and geometric cross sections, 10×10^{-16} m^2 and 10^{-20} m^2 respectively. We measured Landé g factors of 0.34 for Rb87 and 0.50 for Rb85, compared to the theoretical 1/3 and 1/2 respectively. This data was used to calibrate the magnetic sweep field and the main field, and a linear relationship between the main current and the main field was observed. Our results display that optical pumping is an effective technique to investigate the electronic structure of an atom and its isotopes beyond the general energy level splits. (134)

1 Introduction

Optical pumping is a technique used to alter the equilibrium populations of a collection of atoms to perform spectroscopic analysis. The method was developed by A. Kastler and J. Brossel of the Ecole Normale Superieure in Paris, and by Frances Bitter of MIT in the 1950s [1].

Pumping a material involves applying a DC field and perpendicular RF field to a sample cell and firing a circularly polarized photon beam at the atoms. This induces transitions between electronic energy levels and Zeeman levels, distributing electrons among their excited states. Thus the emission spectrum of the material can be observed.

To avoid "leakage" back into the ground states from collisions, Kastler's group developed the preventative methods of introducing buffer gasses into the cell and coating the cell walls with a buffer material. A 2022 research group measured that introducing a buffer gas can into an Rb ensemble can increase optical control by > 25 times [2].

Kastler was awarded the Nobel Prize for his work on optical methods to study resonances. Optical pumping was found to be significantly more sensitive compared with the more inconvenient spectroscopy methods used before Kastler, such as viewing a spectrograph, bringing materials to very low temperatures, or passing a beam of atoms through a magnetic field. Optical pumping continues to be relevant, with a wide variety of applications such as laser technology, atomic clocks and frequency standards, and sensitive measurements of magnetic fields. More recently, optical pumping has been used to enhance Magnetic Resonance Imaging [3].

The purpose of our experiment was to employ this technique to investigate electronic properties of rubidium. Rubidium, like hydrogen, has a single unpaired valence electron that can be brought to excited states. This excitation was achieved through pumping, and we observed the zero-field resonance and Zeeman field splitting of the energy levels. This enabled us to determine the isotopes of rubidium and measure their Landé g factors. We also measured the collision cross-section in the experiment. These measurements revealed properties of the electronic behavior of rubidium and matched our theoretical expectations, confirming optical pumping is an effective measurement technique. This means that moving forward, the technique can be used to analyze more complex atoms with multiple valence electrons.

2 Background

During our first experiment, we measured the cross-section for the collision of photons with our sample of rubidium. The cross-section σ for the absorption of photons by a volume of gas is given by Eq (1),

$$I = I_0 e^{-\sigma_0 \rho l} \tag{1}$$

where I_0 and I represent the incident and outgoing photon flux respectively, ρ is the gas density, and l is the path length through the gas. Here, the incident photons are resonant with an atomic transition, so our experimental cross-section will differ from the geometric cross-section, which is the physical surface area of the collision. Since the geometric cross-section doesn't account for magnetic fields, we expected our experimentally estimated value to be higher than the geometric cross-section.

During our second experiment, we observed the Zeeman resonances of rubidium. The Zeeman effect occurs when a magnetic field is applied to atomic electrons, which also have their own magnetic dipole moment. As a result, the electron acquires an additional energy and some degenerate energy levels will split into several nondegenerate energy levels with different energies.

For example, Fig 1 displays all possible transitions of the Rb87 isotope from 795 nm circularly polarized light.

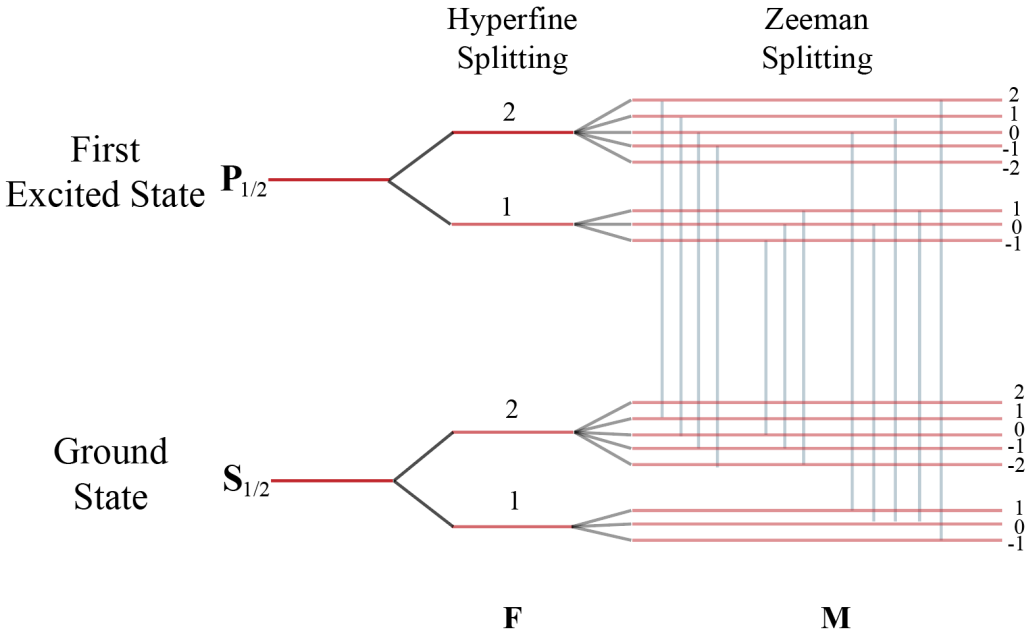

Figure 1: Hyperfine and Zeeman splitting of the $S_{1/2}$ and $P_{1/2}$ levels of Rb87

Splitting can be induced by applying an oscillating RF magnetic field. The resonance frequency v, in units of Hz is calculated by Eq (2),

$$v = g_F \mu_0 B/h \tag{2}$$

where h is Planck's constant, g_F is the Landé g factor, and B is the magnetic field.

3 Methods

3.1 Setup

To conduct optical pumping, we used an optical pumping apparatus from Teachspin, with their supplied external temperature and magnetic field controller. A schematic of the apparatus is shown in Fig 2.

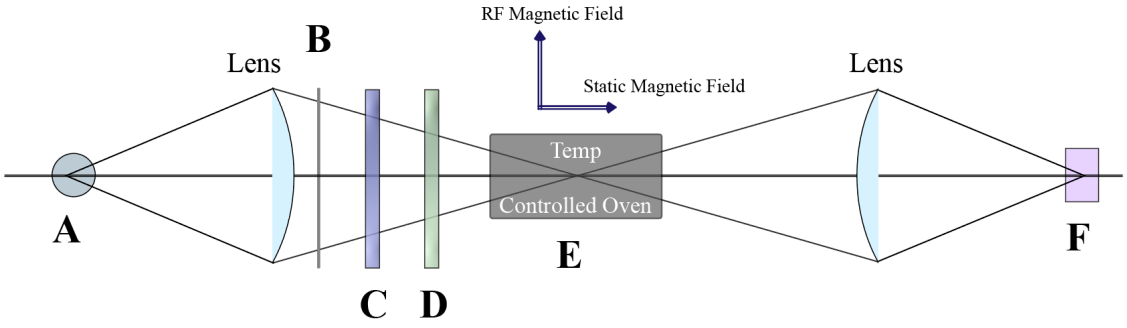

Figure 2: Schematic of optical pumping apparatus used in our experiment

A Rubidium discharge lamp: Emitted resonance light at two main lines, 780 nm and 795 nm

Two plano-convex Lenses: diameter 50 mm, focal length 50 mm.

B 50 mm interference filter used to tune resonance wavelengths

C, D 50 mm linear polarizer at 45° followed by 50 mm quarter wave plate at 0° enable a beam of circularly polarized light to enter the cell.

D Rubidium absorption cell: Consisted of an RF oscillator, oven, and gas bulb filled with rubidium metal and xenon as a buffer gas. The Helmholtz coils around the cell provided a

DC magnetic field along the optical axis. There is also a perpendicularly applied RF field. The coil settings are:

$$\text{Radius} = 0.1639 \text{ m, Turns} = 11 \text{ / side, B(Gauss)} = 8.99 \cdot 10^{-3} \text{ I N / R} \qquad (3)$$

Eq (3) relates the B field from a solenoid given a current I, turn number N, and radius R

E Optical detector PDB-C108: circular 1/4 in diameter diode, connected to voltage preamplifier.

The external controller supplied a static field that was used to cancel the Earth's magnetic field. We first used a compass to position the apparatus pointing north. Then, we slowly swept the horizontal magnetic DC sweep field and observed a dip in intensity from the zero-field absorption line using an oscilloscope. We rotated the apparatus until we achieved the narrowest width of this dip. This process was completed before each experiment.

3.2 Exp A: Absorption of Rb resonance radiation by Atomic Rb

The purpose of this experiment was to approximate the absorption of the rubidium resonance radiation by atomic rubidium, and compare our value to the geometric and theoretical cross-sections.

The linear polarizer (B) and quarter wave plate (C) were removed. The temperature of the cell heater was increased from 300 K to 370 K in steps of 10 K, and allowed to equilibrate at each increment. Measurements of the intensity of the optical signal were recorded at each step using a voltmeter connected to the detector amplifier.

Using accepted values of the density of rubidium as a function of temperature [4], we then determined the cross section for the absorption or rubidium resonance radiation by atomic rubidium.

3.3 Exp B: Low Field Resonances

In these experiments, the rubidium was optically pumped, and the zero-field resonance and Zeeman field splitting were observed. We used the technique to measure the residual field,

determine the g_F values and nuclear spins, and calibrate the sweep and main field.

3.3.1 Nuclear Spins

The linear polarizer and quarter wave plate were reinserted, and the cell temperature set to 320 K. First, to measure the residual field, the main field coils were disconnected and the sweep field coils centered on the zero-field resonance. The current was measured, and with Eq (3), the residual magnetic field was determined.

Then, the RF field was turned set a frequency of 150 kHz. The horizontal magnetic field was swept, and the current at which the Zeeman resonances occurred for Rb85 and Rb87 were observed. The residual field was subtracted from these values to find the calibrated resonance frequencies, and from Eq (2), the g_F values and corresponding nuclear spins were determined.

3.3.2 Low Field Zeeman Effect

The RF frequency was increased from 0-200 kHz in increments of 50 kHz, and the current at which the Zeeman resonances for each isotope remeasured. By plotting frequency as a function of current, we could observe if they were indeed linear in the magnetic field. We could also compare the ratio of their slopes, equivalent to the ratio of the g_F values, to the theoretical value of 1.5, as shown below in section 4.3.

3.3.3 Sweep Field Callibration

To determine a more precise value for the magnetic sweep field, the previous measurements and known g_F values were inputted into Eq (2), and the magnetic field was plotted against the current in the sweep coils and linearly fit.

3.3.4 Main Field Callibration

Our next experiment was to calibrate the main field. The main coils were turned on and connected in the same direction as the sweep coils. The RF frequency was increased from 200 kHz to 1 MHz, and the currents at which resonant frequencies for each isotope were

measured. The sweep coil calibration was used to correct the measured fields for the residual field. Then from Eq (2) and the previous calibrations, a relationship between the main current and main field were plotted and linearly fit.

4 Results and Analysis

4.1 Cross Section

Table 1 shows the recorded detector output voltage as a function of temperature, as well as existing accepted data on the density of rubidium as a function of temperature [3].

T (K)	V (V)	ρ(T) (atom/m^3)
300	2.43	1.1×10^{16}
310	2.22	2.9×10^{16}
320	1.44	7.5×10^{16}
330	0.86	1.8×10^{17}
340	0.36	4.3×10^{17}
350	0.027	8.3×10^{17}
360	-0.134	1.5×10^{18}
370	-0.195	3.7×10^{18}

Table 1: Cell temperature and detector output, 2/1/24. Accepted data on rubidium density as a function of temperature is included.

Above a density of around 370×10^{18} there was no further decrease in the intensity of the transmitted light. The nonzero radiation value comes from the wings of the emission line and from the buffer gas in the discharge lamp. To correct for this a constant detector output voltage of 0.195 V was added to all readings, and then plotted, shown in Fig. 3.

With an absorption path length of 2.5 cm, using Eq (1) we measure $\sigma_0 = 1.2 \times 10^{-16}$ m^2

The value of the cross-section calculated from theory is 10×10^{-16} m^2. The geometric cross-section is 10^{-20} m^2. Our measured cross-section is about 10 times smaller than that calculated from theory. This isn't unreasonable considering the sources of error in the experiment, notably the rapid variation of the density of the rubidium atoms in the cell as a function of temperature. Our result is therefore an approximation. Our observed value is

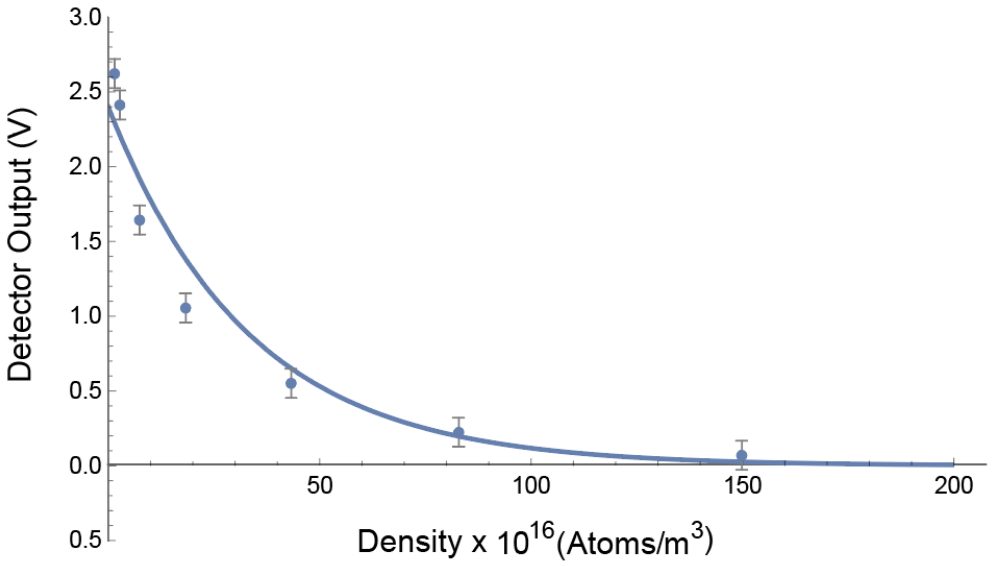

Figure 3: Rubidium Density vs Detector Output, 2/1/24. The exponential line of best fit is $V = 2.40e^{-0.030\rho}$ with $R^2 = 0.9566$

.

larger than the geometric value, as expected.

4.2 Nuclear Spins

The zero field resonance was determined to be at a sweep field current of 0.270 A. Inputting this and the coil parameters into Eq 3, the residual field is calculated to be 0.160 G.

At an RF frequency of 150 kHz the measured currents for the two isotopes were 0.801 A and 0.624 A, corresponding to magnetic field values of 0.483 G and 0.376 G respectively. Subtracting the residual field of 0.160 G yields 0.323 G and 0.216 G.

Using Eq 2 we obtained g_F values of 0.34 and 0.50. When compared with theoretical g_F values of 1/3 and 1/2, our errors are 0.1% and 0% respectively.

4.3 Low Field Zeeman Effect

The currents at which the transition frequencies of each isotope occur as a function of the sweep coil current are given in Table 2.

	I (A)		
f (kHz)	Ground	RB85	RB87
0	0.257	0.257	0.257
100	0.227	0.575	0.463
150	0.274	0.801	0.624
200	0.237	0.936	0.704

Table 2: Sweep Field Calibration

The Rb85 and Rb87 data from Table 2 are plotted in Fig. 4. We observe that the resonances are indeed linear in the magnetic field. We receive a value of 1.5 for the ratio of the slopes, which agrees with the theoretical value of 1.5.

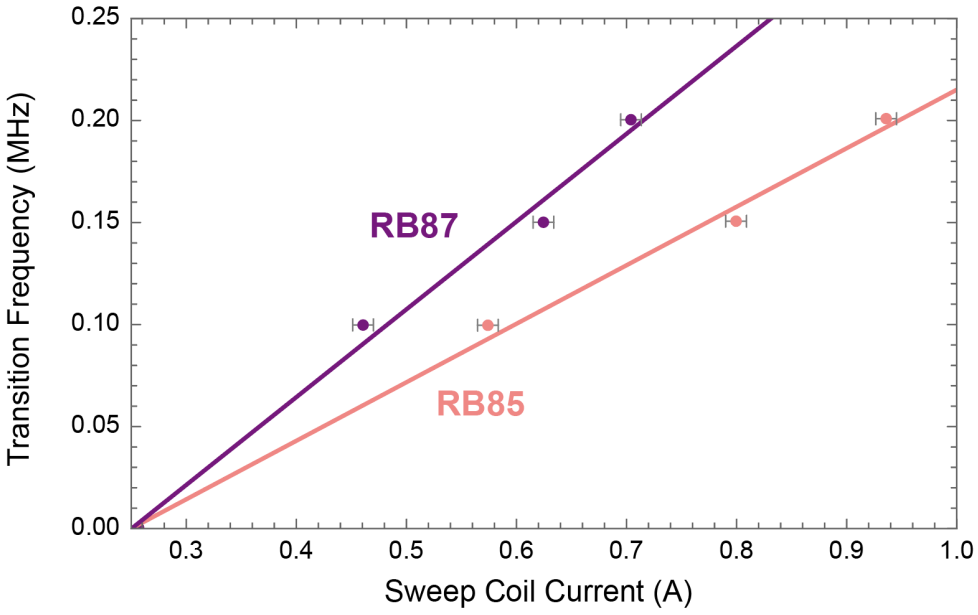

Figure 4: RB85 and RB87 Transition Frequencies, 2/6/24. The linear fit for Rb87 is $v = 0.430\ I - 0.109$ with $R^2 = 0.909618$. The linear fit for Rb85 is $v = 0.287\ I - 0.0717$ with $R^2 = 0.9994278$.

4.4 Sweep Field Callibration

Using the above linear fits for resonance frequency and inputting them into the resonance Eq (2) along with the theoretical g_F values, we calibrated the sweep field. This calibration was observed to be linear, and is shown in Fig. 5.

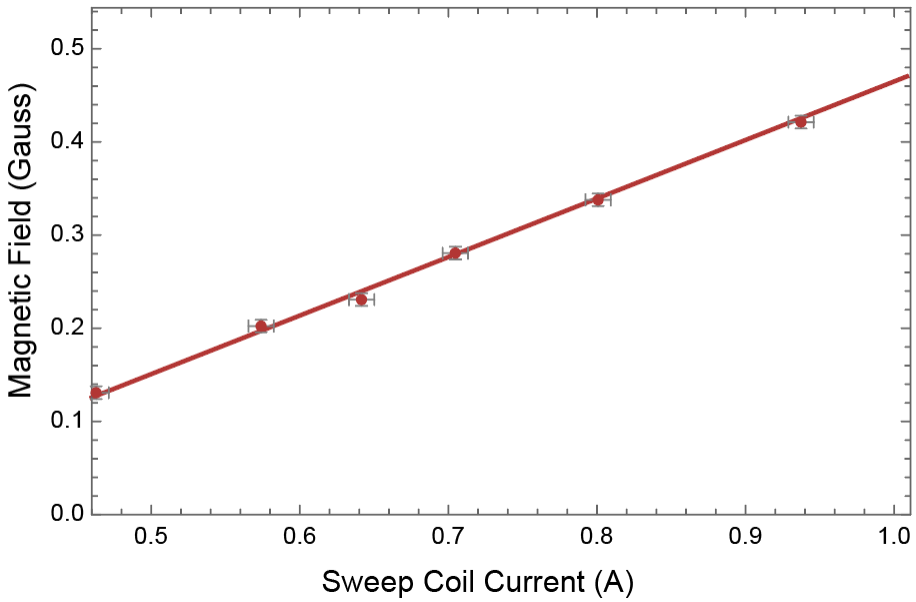

Figure 5: Sweep Field Calibration. The linear fit is $B = 0.620\ I - 0.160$ with $\mathrm{R}^2 = 0.997928$.

4.5 Main Field Callibration

We measured the sweep and main current for each isotope at increasing resonance frequencies, from which we calculated the total field and sweep field with Eq (2). The sweep field calibration and residual field correction were used to find the main B field. These values are shown in Table 3.

We observed a linear relationship between the main field and the main coil current, plotted in Fig 6.

Sources of error in this experiment were introduced by external magnetic fields, precision in alignment with the earth's magnetic field, fluctuation of measurements, and unstable temperature/lack of thermal equilibrium from the heat lamp.

f (MHz)	Total Field (G)	Sweep Current (A)	Main Current (A)	B Field Sweep (G)	B Field Main (G)	Isotope
0.2000	0.283	0.496	0.015	0.147	0.135	RB87
0.2000	0.421	0.730	0.015	0.293	0.130	RB85
0.3000	0.424	0.274	0.031	0.010	0.414	RB87
0.3000	0.632	0.624	0.031	0.227	0.405	RB85
0.4001	0.566	0.484	0.031	0.140	0.426	RB87
0.4001	0.843	0.948	0.031	0.428	0.415	RB85
0.4985	0.705	0.374	0.045	0.072	0.633	RB87
0.4985	1.05	0.927	0.045	0.415	0.636	RB85
1.001	1.41	0.274	0.031	0.242	0.173	RB87

Table 3: Main Field Callibration

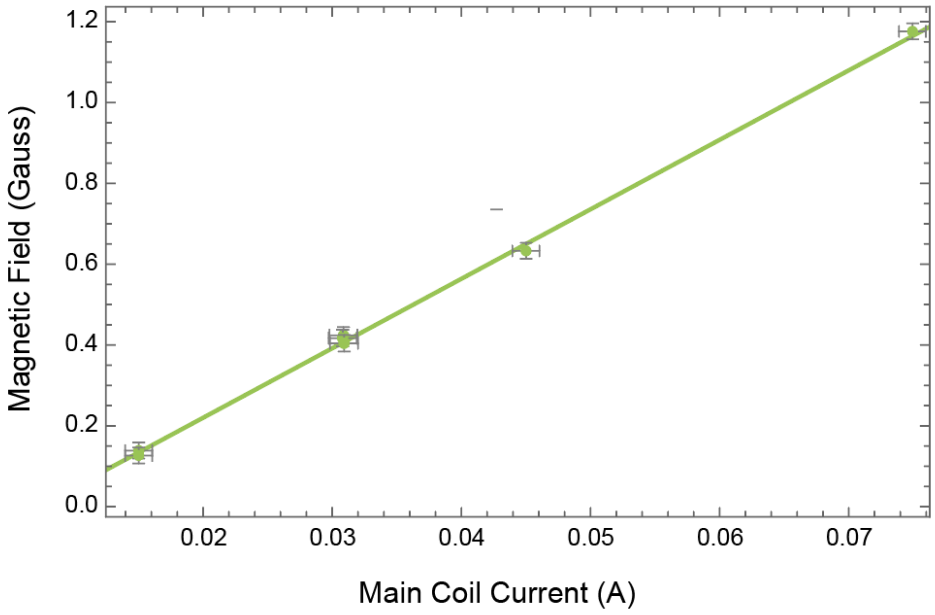

Figure 6: Main Sweep Coils Calibration, 2/20/24. The linear fit is $B = 0.17.2\ I - 0.124$ with $R^2 = 0.998823$

5 Conclusions

We conducted optical pumping of rubidium with a neon buffer gas, in a heat-controlled cell surrounded by Helmholtz coils to apply a DC field, and an RF field.

We measured the beam intensity as a function of temperature and used accepted data on the density of rubidium as a function of temperature to approximate the collision cross-section,

obtaining a value of 1.2×10^{-16} m^2. Compared with the theoretical value 10×10^{-16} m^2, we have an error of 88%. Rapid variation of the density of the rubidium atoms as a function of time is likely the leading source of this error around an order of magnitude. As expected, our estimate was larger than the geometric cross-section, which is 10^{-10} m^2.

We then inserted optical components to circularly polarize the light and observed the zero field transition. We found the residual field to be 0.160 G. With the RF frequency fixed at 150 kHz, we swept the horizontal magnetic field and observed the Zeeman resonances for Rb87 and Rb85. We found g_F values of 0.34 and 0.50, compared with the theoretical 1/3 and 1/2 respectively.

We also plotted the transition frequencies of each isotope as a function of sweep coil current, and found a linear relationship between them. The ratio of their slopes was 1.5, which matched the theoretical value of 1.5.

Using this data and the theoretical g_F values, we calibrated the sweep field and determined a linear relationship between sweep coil current and field.

Lastly, with the main coils connected, we made measurements of the currents at resonance frequencies from 200 kHz to 1 MHz, and used the sweep field calibration to determine the main field. We also found a linear relationship between the main coil current and main field. Our experimentally determined values overall matched our theoretical expectations, showing optical pumping is an effective technique for measuring electronic properties of an element.

References

[1] Optical Pumping A. Bloom. Scientific American. **203.4**, 72 (1960).

[2] Optical pumping and relaxation of atomic population in assorted conditions, S. Pradhan, S. Chowdhury. Journal of Physics B: Atomic, Molecular and Optical Physics **55** 165502 (2022).

[3] Hyperpolarized xenon for NMR and MRI applications, C. Witte, M. Kunth, J. Döpfert, F. Rossella, L. Schröder. Journal of Visualized Experiments, **67** 4268 (2012).

[4] Values of density calculated from the vapor pressure data tabulated in "The Characterization of High Temperature Vapors", (John Wiley & Sons, 1967).